

Investigation of dye-doped red emitting organic electroluminescent devices with metal-mirror microcavity structure

X. Y. Sun, W. L. Li, Z. R. Hong, H. Z. Wei, F. X. Zang et al.

Citation: *J. Appl. Phys.* **97**, 103112 (2005); doi: 10.1063/1.1913794

View online: <http://dx.doi.org/10.1063/1.1913794>

View Table of Contents: <http://jap.aip.org/resource/1/JAPIAU/v97/i10>

Published by the [American Institute of Physics](#).

Additional information on J. Appl. Phys.


Journal Homepage: <http://jap.aip.org/>

Journal Information: http://jap.aip.org/about/about_the_journal

Top downloads: http://jap.aip.org/features/most_downloaded

Information for Authors: <http://jap.aip.org/authors>

ADVERTISEMENT



Special Topic Section:
PHYSICS OF CANCER

Why cancer? Why physics? [View Articles Now](#)

Investigation of dye-doped red emitting organic electroluminescent devices with metal-mirror microcavity structure

X. Y. Sun

Key Laboratory of Excited State Processes, Changchun Institute of Optics, Fine Mechanics and Physics, Chinese Academy of Sciences, 16-Dong Nan Hu Road, Economic Development Area, Changchun, Jilin 130033, People's Republic of China and Graduate School of Chinese Academy of Sciences, Beijing, 100101, People's Republic of China

W. L. Li,^{a)} Z. R. Hong, H. Z. Wei, F. X. Zang, L. L. Chen, Z. Shi, D. F. Bi, and B. Li

Key Laboratory of Excited State Processes, Changchun Institute of Optics, Fine Mechanics and Physics, Chinese Academy of Sciences, 16-Dong Nan Hu Road, Economic Development Area, Changchun, Jilin 130033, People's Republic of China

Z. Q. Zhang and Z. Z. Hu

Organic Photoelectronic Material Research and Development Center, Anshan University of Science and Technology, Anshan, Liaoning 110044, People's Republic of China

(Received 6 July 2004; accepted 24 March 2005; published online 13 May 2005)

Organic electroluminescent (EL) devices with planar microcavity structure, indium-tin-oxide/Ag/N,N'-diphenyl-N, N'-bis(3-methylphenyl)-1,1'-biphenyl-4,4'-diamine/tris(8-hydroxyquinoline)-aluminum (AlQ):4-(dicyanomethylene)-2-methyl-6-(p-dimethyl aminostyryl)-4H-pyran/AlQ/LiF/Al, were fabricated. The Ag and Al layers acted as not only hole-injection layer and cathode, respectively, but reflective mirrors, resulting in strong microcavity effects, such as spectral narrowing and directional emission. The effects of device parameters on the EL performance were studied in detail and were discussed in terms of conventional microcavity theory. On-axis light magnification with a coefficient (EL enhancement ratio between cavity and noncavity devices) of ~ 5 was observed, which was consistent with the theoretical calculation. At the same time, optimized microcavity device with bright pure red emission showed maximum luminance of 5140 cd/m², peak at 624 nm, Commission International de l'Eclairage coordinates of $x=0.663$ and $y=0.336$, and high EL efficiency of 1.71 cd/A were obtained. © 2005 American Institute of Physics. [DOI: 10.1063/1.1913794]

I. INTRODUCTION

Varieties of organic materials and device structures have been studied since Tang and Van Slyke reported the high efficiency double-layer organic light-emitting diodes¹ (OLEDs) and impressive strides have been made in understanding the mechanism of the fundamental phenomena involved as well as in the radiative recombination of carriers on electrically excited organic molecules.² The popularity of OLEDs is also expected to extend to various applications, such as organic transistors, solar cells, and memory devices, especially for the organic laser diodes (OLDs). There have been previous reports on amplified spontaneous emission under optical pumping,³ however, the electrically pumped OLDs have not been realized.⁴ Planar microcavity structures have revolutionized the design of OLEDs, since in the devices with microcavity structures, the photon density of states is redistributed, leading to certain cavity modes, which provides narrow-band emission and color selectivity over a wide range of wavelengths. Therefore, planar microcavity devices attracted much attention recently, and great progress has been made in organic microcavity diodes.^{5–13}

A planar microcavity consists of two parallel mirrors,

forming a Fabry–Pérot resonator. There are two types of mirrors commonly used in electroluminescent (EL) microcavity systems. One is distributed Bragg reflectors (DBRs), which consists of alternating layers with different refractive indices. In spite of the perfect selective reflectivity, the fabrication procedure of DBRs is rather complicated, and additional electrodes are needed because of its insulating property. An alternative is to use semitransparent conductive metal mirror, which is highly reflective over a wide range of wavelengths and can be easily prepared by vacuum thermal evaporation. However, only a few groups have studied the EL characteristics of the device with the latter structure.^{5,6}

Although high efficient blue and green OLEDs have been demonstrated,^{14,15} there has been lack of devices that exhibit both saturated red emission and high EL efficiency. Many fluorescent dyes and their derivatives have been employed, such as 4-(dicyanomethylene)-2-methyl-6-(p-dimethyl aminostyryl)-4H-pyran (DCM1) (Ref. 16) and 4-(dicyanomethylene)-2-t-butyl-6-(1,1,7,7-tetramethyljulolidyl-9-enyl)-4H-pyran (DCJTb),¹⁷ however, pure red EL requires relatively high dopant concentration, which causes serious self-quenching and decreases EL efficiency. Narrow-band red emission was achieved in OLEDs with europium complexes, while the EL performance needs further improvement.^{18,19}

In this paper, triple-layer devices with metal-mirror mi-

^{a)}Author to whom correspondence should be addressed; electronic mail: wllioel@tom.com

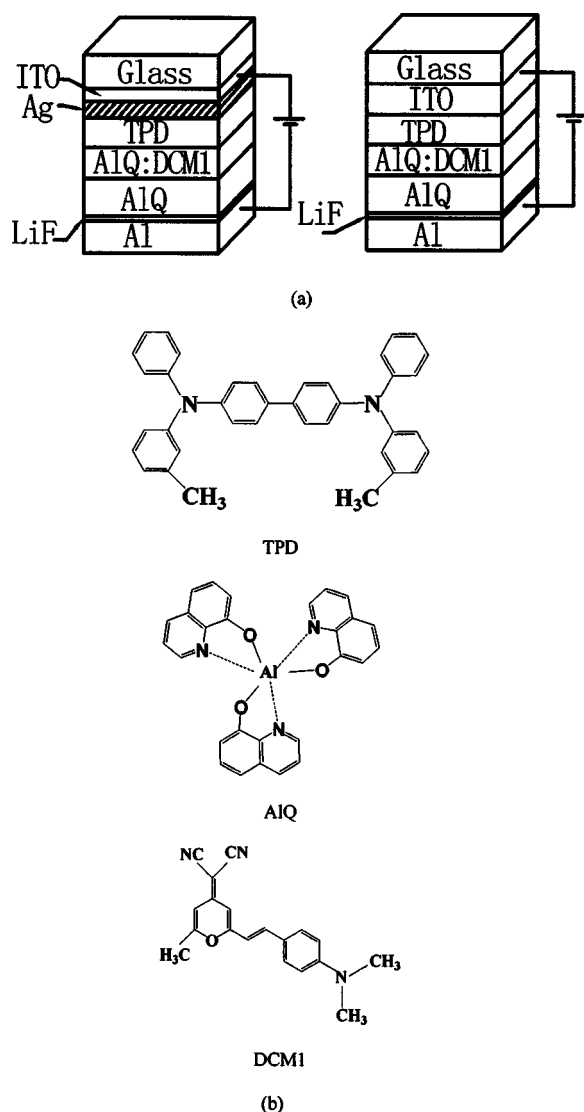


FIG. 1. (a) Schematic illustration of device structures, cavity device (left), and control device (right); (b) molecular structures of organic materials used.

microcavity structure based on DCM1-doped tris(8-hydroxyquinolino)-aluminum (AIQ) were studied. The EL characteristics of the microcavity devices, including the carrier injection, the emission surface, the dependence of emission peak on detection angle (θ), as well as the relationship between the dopant concentration and the EL efficiency, were discussed in detail. Finally, efficient pure red EL was obtained in the optimal device.

II. EXPERIMENT

Device configurations and molecular structures of organic materials used are shown in Figs. 1(a) and 1(b), respectively. In cavity device, semitransparent Ag anode and Al cathode (200 nm) were employed as two reflectors. Sandwiched between the mirrors were hole transporting layer N,N'-diphenyl-N,N'-bis(3-methylphenyl)-1,1'-biphenyl-4,4'-diamine (TPD), emitting layer DCM1 doped in AIQ, and electron transporting layer AIQ. A 0.5-nm LiF layer was combined with Al for efficient electron

injection. Control devices (without Ag mirror) were also fabricated during the same vacuum run for comparison. All the devices were constructed on indium-tin-oxide (ITO) coated glass substrate with a sheet resistance of $130 \Omega/\text{sq}$. All the metal and organic layers were deposited by vacuum thermal evaporation at a pressure of 5×10^{-4} Pa, and the deposition rate was about 0.05 nm/s. After the deposition of the Ag film, the substrates were exposed in air for patterning process. The light output was observed from the semitransparent Ag side. The emission area was $2 \times 4 \text{ mm}^2$. The EL spectra were detected by a Hitach-4000 fluorescence spectrophotometer. The brightness and carrier injection characteristics were recorded by a calibrated multifunctional system for EL measurement. The thickness of the films was measured by an atomic force microscope, and the transmittance of Ag mirror was measured by a UV-3101 personal computer (PC). All the measurements were carried out in atmosphere at room temperature.

III. RESULTS AND DISCUSSION

A. The effect of the thicknesses of Ag mirror on device performances

The transmittance of Ag mirrors with the thicknesses of 15, 28, and 33 nm are about 34%, 25%, and 17% at $\lambda = 630 \text{ nm}$, respectively. Neglecting light scattering and absorption, the reflectivities are 66%, 75%, 83%, respectively. In fact, the 15-nm Ag film suffers serious surface oxidation and its reflectivity is lower than 66%.

The thicker of the Ag mirror, the higher of the reflectivity, resulting in the stronger cavity effect, which is required by the monomode resonance. Meanwhile, much thicker Ag mirror decreases the EL output intensity. The tradeoff of the two paradox parameters is critical for achieving highly efficient microcavity EL devices. To realize optimum the thickness of Ag mirror, the I - V characteristic, and the EL spectrum of cavity devices with different thickness of Ag were measured, and the results are shown in Figs. 2(a) and 2(b), respectively. Comparing the cavity devices with noncavity device, the hole injection from Ag anode into TPD layer is inefficient due to its large energy gap.²⁰ The device with 15-nm Ag anode exhibits the best hole injection among the three cavity devices, which is explained that thinner Ag film is easily oxidized to Ag_2O , and the Ag_2O film appears to match with TPD, giving good anode contact.²⁰ For the thicker Ag films, better surface uniformity leads to better hole injection, thus, the 33-nm Ag anode has more efficient hole injection than that of the 28-nm Ag anode.²⁰

In Fig. 2(b), it is noticed that the device with 15-nm Ag mirror narrows the emission spectrum slightly, and the full width at half maximum (FWHM) changes from 70 nm (in noncavity device) to 60 nm (in cavity device), which is attributed to the low reflectivity of the 15-nm Ag mirror and leading to the weak cavity effect as mentioned above. The 28-nm and 33-nm Ag mirrors narrow the spectra considerably, and the FWHMs reach 40 and 30 nm, respectively. Considering the hole-injection characteristic and the spectral narrowing effect, 33-nm Ag mirror is selected in this study.

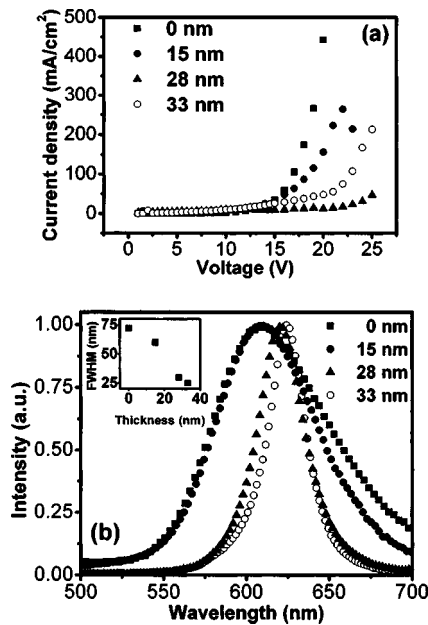


FIG. 2. (a) The normalized emission spectra of EL devices with different thickness of Ag mirror; (b) I - V curves of EL devices with different thickness of Ag mirror.

B. The effect of cavity length on EL peak

The resonant modes in a cavity can be tuned by altering the medium thickness, i.e., the cavity length.

Increasing the thickness of organic layer, redshift of emission peak is observed in cavity devices, as shown in Fig. 3. When the dopant (DCM1) concentration is 0.76 mol % and the cavity length increases from 115 to 148 nm, the emission peak shifts from 577 to 706 nm. In contrast, the emission peak of control devices still remains at 607 nm. For simplicity, the emission angle at normal direction of the cavity device is assumed to be the detection angle, and then the resonance condition for the cavity device with emission peak at λ is expressed by Eq. (1),

$$\sum 2n_i l_i \cos \theta + \frac{\lambda}{2\pi} \Delta\varphi = m\lambda, \quad (1)$$

where n_i and l_i represent the refractive index and thickness of the i th layer, respectively, θ represents the outer emission angle, $\Delta\varphi$ is the sum phase change at the two organic/metal interfaces, and m is the mode index. When the maximum resonant emission was achieved, m was a nonzero integer.

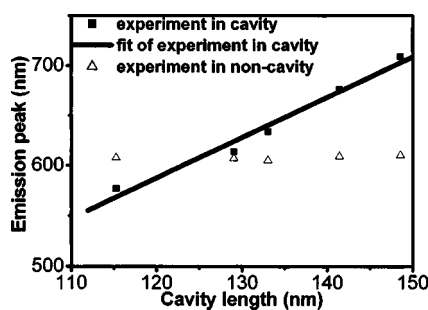


FIG. 3. The emission peak vs the cavity length and the linear fitting of experiment values of cavity devices.

Usually the refractive index of organic layers in the emission wavelength region is 1.7. The $m=1.1$ is obtained by linearly fitting the experimental values, which is close to the theoretical value.

C. Light magnifying in cavity devices

The brightness of noncavity device with 0.76 mol % DCM1:ALQ is 1620 cd/m^2 at 125 mA/cm^2 . If on-axis cavity effect did not exist, the brightness of cavity device should be 280 cd/m^2 (considering the transmittance of 33-nm Ag mirror). But actually, the brightness of 1500 cd/m^2 is achieved, which is 5.3 times higher than 280 cd/m^2 . If the quenching effect of Ag mirror on the EL emission was taken into account, the magnification coefficient ($G_m = G_{\text{cav}}/G$) should be more than 5.3.

On the other hand, theoretical estimation of the resonant emission enhancement factor G_{cav} ,

$$G_{\text{cav}} = \frac{\xi (1 + \sqrt{R_2})^2 (1 - R_1)}{2 (1 - \sqrt{R_1 R_2})^2} \frac{\tau_{\text{cav}}}{\tau}, \quad (2)$$

where R_1 represents the reflectivity of Ag mirror (for cavity devices) or ITO (for noncavity devices), R_2 is the reflectivity of Al electrode, τ_{cav}/τ is the molecular excited-state lifetime in the cavity divided by the free-space molecular excited state, and $\xi/2$ is the field strength at the emission position relative to the free-space field strength. The resonant structure (624-nm mode) has $R_{\text{Al}}=0.83$, $R_{\text{ITO}}=0.04$, and $R_2=0.90$. Assuming $\tau_{\text{cav}}/\tau=0.9$ (Ref. 21) and $\xi=1$, the G_m is ~ 6 , which is consistent with the experimental value.

D. The effect of dopant concentration on the performance of EL devices

At a definite cavity length, the EL characteristics, such as EL spectrum, luminescence efficiency, and Commission International de l'Eclairage (CIE) coordinates of cavity device, are strongly influenced by dopant concentration. When the cavity length is fixed at 133 nm, the resonant wavelength is 624 nm.

Figure 4(a) shows the dopant concentration (varied from 0 to 1.63 mol %) dependence of the emission peak and EL efficiency at 20 mA/cm^2 . For noncavity devices, the highest efficiency with 0.27 mol % dopant concentration is induced by the direct radiative recombination on DCM1, and the decreased efficiency at high dopant concentration is ascribed to concentration quenching. However, for cavity devices, the EL efficiency increases with increasing dopant concentration at first, and the maximum EL efficiency is achieved at dopant concentration of 0.76 mol %. This finding should be ascribed to the competition between the concentration quenching and the light magnifying. That is, at low dopant concentration of 0 or 0.27 mol %, light magnifying effect in cavity devices is not pronounced due to the mismatch between the spontaneous emission peak and the resonant wavelength. When the resonant wavelength coincides with the spontaneous emission by increasing dopant concentration up to 0.76 mol %, both efficient spontaneous emission and effective light mag-

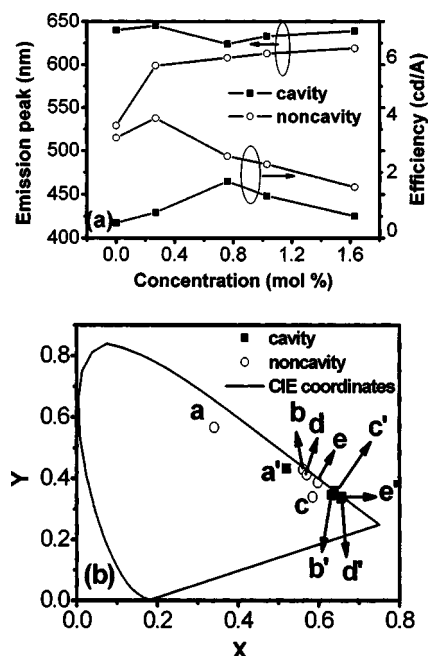


FIG. 4. (a) The emission peak and EL efficiency vs the dopant concentration; (b) the CIE coordinates of EL devices with different dopant concentration (*a-e* and *a'-e'* represent the noncavity and cavity devices with dopant concentration increasing from 0 to 1.63 mol %, respectively).

nification result in the highest EL efficiency. When the concentration exceeded 1 mol %, the quenching effect becomes obvious, and the EL efficiency decreases.

Figure 4(b) shows the dependence of the CIE coordinates on dopant concentration for two types of devices. All the devices gradually approach to red region with increasing dopant concentration. For noncavity devices, the emission-peak redshift with increasing dopant concentration due to strong polarization effect²² brings more saturated red light emission. However, the emission color of highest dopant concentration is still in orange-red region. For cavity devices, the pure red emission can be observed from doped devices, and this is the result of strong resonant effect.

E. The dependence of EL spectra and emission pattern on detection angle

Figure 5(a) depicts the dependence of the emission peak on the detection angle (θ) of cavity device with 133-nm cavity length and 0.76 mol % dopant concentration. With increasing detection angle, the emission peak shifts to blue obviously, this could be explained by Eq. (1).

It is interesting that the difference between resonant wavelength (λ_{cav}) and spontaneous emission peak (λ_{non}), i.e., $\Delta\lambda = \lambda_{\text{cav}} - \lambda_{\text{non}}$, significantly affects the EL performance of cavity device. For each parallel comparison, λ_{non} is ~ 610 nm and λ_{cav} is tuned by the thickness of organic layers, and then obtain the $\Delta\lambda$ of 0.6, 24.8, and 48 nm, respectively.

The emission pattern of noncavity device is uniform spatial distribution nearly Lambertian, as shown in Fig. 5(b). Figure 5(b) also shows the emission pattern of cavity devices with different $\Delta\lambda$. It is clear that the resonant emission is strongly directed along a certain angle. The strongest outer

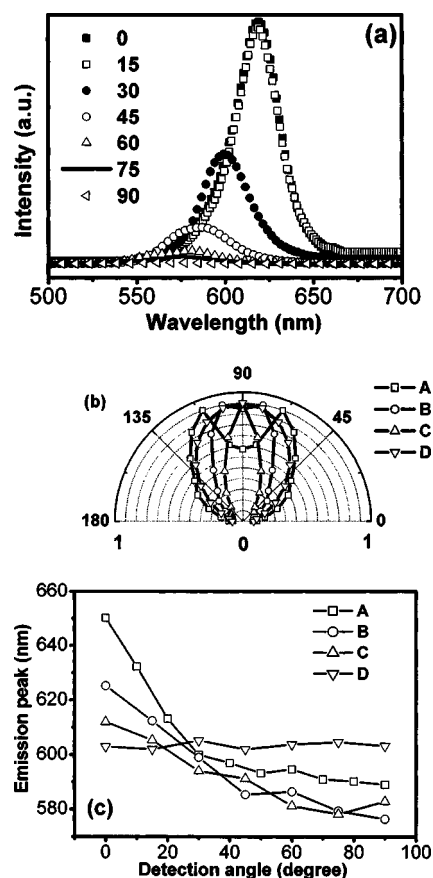


FIG. 5. (a) The EL spectra detected at different angle; (b) the emission surface varied with the $\Delta\lambda$ and the ideal emission surface from noncavity device; (c) dependence of wavelength shift on detection angle with different $\Delta\lambda$. [Device A, B, and C in (b) and (c) represent the microcavity devices with $\Delta\lambda$ of 48, 24.8, and 0.6 nm, respectively; device D represents the noncavity device.].

emission angle is increased with increasing $\Delta\lambda$, which should also be attributed to the match of the resonant condition and the spontaneous emission.

Figure 5(c) shows the dependence of the emission peak on detection angle. The emission peak of noncavity device does not vary with increasing detection angle, while the EL peak shifts to blue with increasing θ from 0° to 45° for the three cavity devices. For $\Delta\lambda = 0.6, 24.6$, and 48 nm, blue-shifts of 21, 40, and 55 nm are observed, respectively. With increasing $\Delta\lambda$, the blueshift upon detection angle becomes intensive. The EL peaks range from 580 to 595 nm with detection angle $> 45^\circ$, since the spontaneous emission from DCM1 < 580 nm is weak.

F. The pure red high-efficiency EL from cavity device

Using microcavity structure, efficient pure red EL device is achieved. For comparison, the cavity and noncavity device consist of the same active layer (0.76 mol % DCM1 doped in AlQ and 133-nm cavity length). In cavity device, the maximum efficiency of 1.71 cd/A and luminance of 5140 cd/m² are obtained, respectively, as is shown in Fig. 6(a). Although for noncavity device, the maximum efficiency and luminance are 2.12 cd/A and 6220 cd/m², respectively, the emission color is still orange red. Figure 6(b) plots the normal EL

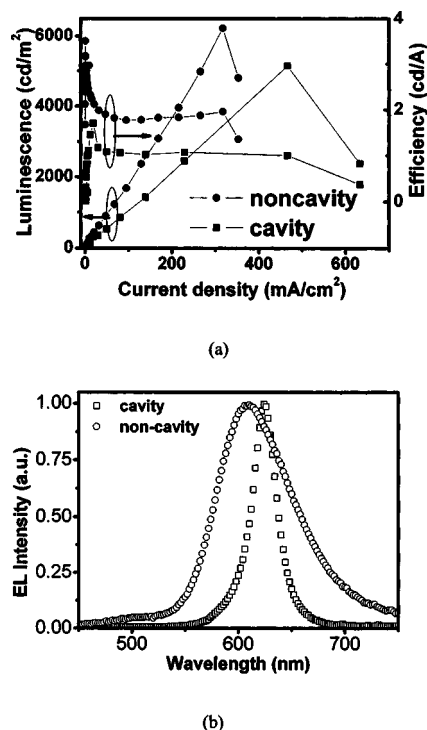


FIG. 6. (a) Luminescence and EL efficiency vs current density for cavity and noncavity device of 0.76 mol % dopant concentration; (b) the normalized EL spectra for cavity and noncavity device of 0.76 mol % dopant concentration.

spectra of the cavity and noncavity device. It was found that 624-nm EL emission peak with the FWHM of 26 nm from cavity device is obtained. And for the control device, the EL emission peak at 610 nm with FWHM of 87 nm is observed. Besides, the emission from AlQ is suppressed completely in cavity device. Therefore, it is demonstrated that our optimal cavity device shows saturated red emission ($x=0.655$ and $y=0.336$), closing to the National Television Standards Committee recommended red for a video display.

IV. CONCLUSION

The microcavity devices with Ag and Al mirrors were fabricated. Comparing the EL characteristics of cavity and noncavity devices provided an evidence for strong light magnification effect. It was found that in cavity devices the thick-

ness of Ag mirror had considerable influence on the EL performance. The efficient EL emission can be obtained by optimizing dopant concentration. Besides, it was found that deviation of strongest EL emission direction from normal increased with increasing $\Delta\lambda$. On the other hand, pure red emission, high luminance, and efficiency were obtained in cavity device, which provides a method for achieving pure red primary color of full color displays. The EL emission can be tuned by varying the detection angle and the cavity length, which is promising for special display applications, such as directional display.

ACKNOWLEDGMENT

This work is in part supported by the National Science Research Project (Project No. 90201012) of China.

- ¹C. W. Tang and S. A. Van Slyke, *Appl. Phys. Lett.* **51**, 913 (1987).
- ²J. Szmytkowski, W. Stsmpor, J. Kalinowski, and Z. H. Kafafi, *Appl. Phys. Lett.* **80**, 1465 (1987).
- ³V. G. Kozlov *et al.*, *Appl. Phys. Lett.* **84**, 4096 (1998).
- ⁴M. A. Baldo, R. J. Holmes, and S. R. Forrest, *Phys. Rev. B* **66**, 035321 (1998).
- ⁵H. Becker, S. E. Burns, N. Tessler, and R. H. Friend, *J. Appl. Phys.* **81**, 2825 (1997).
- ⁶N. Takada, T. Tsutsui, and S. Saito, *Appl. Phys. Lett.* **63**, 2032 (1993).
- ⁷R. H. Jordan, L. J. Rothberg, A. Dodabalapur, and R. E. Slusher, *Appl. Phys. Lett.* **69**, 1997 (1996).
- ⁸A. Dodabalapur, L. J. Rothberg, R. H. Jordan, T. M. Miller, R. E. Slusher, and J. M. Phillips, *J. Appl. Phys.* **80**, 6954 (1996).
- ⁹A. Dodabalapur, L. J. Rothberg, T. M. Miller, and E. W. Kwock, *Appl. Phys. Lett.* **64**, 2486 (1994).
- ¹⁰T. Tsutsui, N. Takada, and S. Saito, *Appl. Phys. Lett.* **65**, 1868 (1994).
- ¹¹A. Dodabalapur, L. J. Rothberg, and T. M. Miller, *Appl. Phys. Lett.* **65**, 2308 (1994).
- ¹²T. Tsutsui, N. Takada, and S. Saito, *Appl. Phys. Lett.* **63**, 2032 (1993).
- ¹³T. A. Fisher, D. G. Lidzey, M. A. Pate, M. S. Weaver, D. M. Whittaker, M. S. Skolnick, and D. D. C. Bradley, *Appl. Phys. Lett.* **67**, 1355 (1995).
- ¹⁴C. H. Chen and C. W. Tang, *Appl. Phys. Lett.* **79**, 3711 (2001).
- ¹⁵J. Shi and C. W. Tang, *Appl. Phys. Lett.* **80**, 3201 (2002).
- ¹⁶J. Littman and P. Martic, *J. Appl. Phys.* **72**, 1 (1992).
- ¹⁷T. H. Liu, C. Y. Iou, S. W. Wen, and C. H. Chen, *Thin Solid Films* **441**, 223 (2003).
- ¹⁸C. Adachi, M. A. Baldo, and S. R. Forrest, *J. Appl. Phys.* **87**, 8049 (2000).
- ¹⁹Z. R. Hong *et al.*, *Adv. Mater. (Weinheim, Ger.)* **13**, 1241 (2001).
- ²⁰C. W. Chen, P. Y. Hsien, H. H. Chiang, C. L. Lin, H. M. Wu, and C. C. Wu, *Appl. Phys. Lett.* **83**, 5127 (2003).
- ²¹M. Osuge and K. Ujihara, *J. Appl. Phys.* **76**, 2588 (1994).
- ²²H. Ishii, K. Sugiyama, E. Ito, and K. Seki, *Adv. Mater. (Weinheim, Ger.)* **11**, 605 (1999).